RESEARCH ARTICLE

AMERICAN JOURNAL OF medical genetics PART A

Increase in Central Striatal Dopamine Transporters in Patients With Shwachman–Diamond Syndrome: Additional Evidence of a Brain Phenotype

Jan Booij,[1] Liesbeth Reneman,[2] Marielle Alders,[3] and Taco W. Kuijpers[4]*

[1]Department of Nuclear Medicine, Academic Medical Center, University of Amsterdam, Amsterdam, The Netherlands

[2]Department of Radiology, Academic Medical Center, University of Amsterdam, Amsterdam, The Netherlands

[3]Department of Clinical Genetics, Academic Medical Center, University of Amsterdam, Amsterdam, The Netherlands

[4]Emma Children's Hospital, Academic Medical Center, University of Amsterdam, Amsterdam, The Netherlands

Manuscript Received: 12 April 2012; Manuscript Accepted: 3 September 2012

Patients with Shwachman–Diamond syndrome (SDS) do not only experience well-described physical features like skeletal abnormalities and hematological dysfunctions, but recent studies also suggested attention and working memory deficits in SDS. Indeed, a recent structural magnetic resonance imaging (MRI) study demonstrated smaller brain regions in SDS. Regarding attention and working memory, however, an important role for the neurotransmitter dopamine is well established. Therefore, in this study we assessed in vivo dopamine transporters (DATs; a specific marker of dopaminergic cells expressed in nerve terminals) and performed structural MRI in SDS. In 6 and 5 young SDS patients, respectively, we were able to acquire DAT single photon emission computed tomography (SPECT) and MRI examinations, and the data were compared to age-matched control data. Striatal DAT binding was significantly increased in SDS patients as compared to controls. In addition, we observed significantly smaller volumes particularly posteriorly and caudally located in the brain: the corpus callosum, brainstem, and cerebellum. Also the thalamus was smaller in SDS patients than in controls. In conclusion, our data replicate earlier findings on smaller brain regions in SDS. In addition, our novel molecular imaging data suggest that SDS patients may have a dysregulated dopaminergic system. These findings may be of relevance to increase our understanding of behavioral and cognitive deficits in SDS. © 2012 Wiley Periodicals, Inc.

Key words: Shwachman–Diamond syndrome; MRI; dopamine; SPECT; attention

How to Cite this Article:
Booij J, Reneman L, Alders M, Kuijpers TW, 2013. Increase in central striatal dopamine transporters in patients with Shwachman–Diamond syndrome: Additional evidence of a brain phenotype.
Am J Med Genet Part A 161A:102–107.

INTRODUCTION

Clinical characteristics of the rare autosomal-recessive Shwachman–Diamond syndrome (SDS) are exocrine pancreatic dysfunction, short stature, skeletal abnormalities, and hematological dysfunction (typically neutropenia), but additional organ systems, such as the liver, may be affected as well [Huang and Shimamura, 2010; Dror et al., 2011]. SDS results from mutations in the Shwachman–Bodian–Diamond (*SBDS*) gene on chromosome 7q11 [Boocock et al., 2003]. A genotype–phenotype relationship has not been established to date [Kuijpers et al., 2005]. Although the hematological abnormalities and pancreatic insufficiency are the main clinical hallmarks of SDS, the disease may present otherwise in a highly variable manner in the presence of the two or three most common biallelic mutations identified [Huang and Shimamura, 2010]. The protein has a role in ribosome processing [Finch et al., 2011] and has recently been grouped together with other (hematological) bone marrow failure syndromes as a ribosomopathy [Narla and Ebert, 2010]. Most likely the role of SBDS is multifunctional, being not only associated with the 60S preribosomal precursor subunit involved in polysome formation, but also found to localize to the tubulin-containing mitotic spindle [Austin et al., 2008; Orelio et al., 2009] as well as the F-actin-containing cytoskeleton of motile cells [Orelio and Kuijpers, 2009]. When mutated, the patient-derived SBDS is strongly reduced in expression levels but not completely absent. However, its intracellular

The other authors declared that they have no conflict of interest.
J.B. is consultant at GE Healthcare.

*Correspondence to:
Taco W. Kuijpers, M.D., Ph.D., Emma Children's Hospital, Academic Medial Center, University of Amsterdam, Amsterdam, The Netherlands.
E-mail: t.w.kuijpers@amc.uva.nl

Article first published online in Wiley Online Library (wileyonlinelibrary.com): 14 December 2012
DOI 10.1002/ajmg.a.35687

localization has clearly changed [Orelio et al., 2011; Yamaguchi et al., 2011].

SBDS is expressed in all organs, including the brain [Boocock et al., 2003]. In this regard, it is becoming increasingly apparent that many SDS patients also suffer from behavioral problems and cognitive dysfunction including learning difficulties [Toiviainen-Salo et al., 2008; Perobelli et al., 2012]. A recent preliminary study suggested that a number of SDS patients also experience attention deficits [Kerr et al., 2010].

Structural MRI demonstrated smaller brain regions in SDS, particularly the corpus callosum, cerebellar vermis, posterior fossa, and brainstem [Toiviainen-Salo et al., 2008]. The observed reduced sizes of brain regions, and particularly the cerebellum, was suggested to be related to cognitive dysfunctions in SDS [Toiviainen-Salo et al., 2008].

Regarding attention and working memory an important role for the neurotransmitter dopamine is well established [Williams and Goldman-Rakic, 1995; for a review see Klingberg, 2010]. The dopamine transporter (DAT) is a protein that is expressed exclusively in the cell membrane of dopaminergic neurons, playing a key role in the reuptake of dopamine from the synaptic cleft. With novel molecular imaging techniques (SPECT or PET) it is feasible to visualize and quantify DATs in the living human brain [Booij et al., 1997, 1999, 2007, 2010]. An increased availability of dopamine transporters (DATs) has been reported in the striatum of patients suffering from attention-deficit hyperactivity disorder (ADHD) [Dougherty et al., 1999].

In this study, we examined the expression of striatal DAT in SDS patients and controls, combined with neuroimaging of the brain with structural MRI.

MATERIALS AND METHODS

Patients

We included six SDS cases (4 males and 2 females; mean age: 18.5 years, range: 12–26 years) for structural MR and SPECT imaging (Table I). All cases had a clinical diagnosis of SDS and were compound heterozygous for *SBDS* gene mutations commonly identified in SDS (Table I).

Accurate brain MRI data could be obtained in five cases (Table I; mean age: 18.6 years, range: 12–26 years) and were compared to those obtained in 6 healthy age- and gender-matched controls (2 males and 4 females; mean age: 16.2 years, range: 12–21 years). These teenagers had undergone brain MRI as requested by pediatric neurologists because of complaints of persistent headaches. Imaging, electroencephalography (EEG) and 6 months of clinical follow-up data were available to exclude the presence of any obvious, underlying neurological pathology. The study was approved by the local medical ethics committee of the Academic Medical Center, Amsterdam.

MRI Image Acquisition and Analysis

We acquired high resolution sagittal 3D spoiled gradient echo sequences covering the whole head (T1W, TR/TE = 9/53 msec, FOV 232 mm × 256 mm, 170 slices voxel size 0.9 × 1.0 × 1.0 mm^3) on 1.5 T MRI scanners in all subjects, except for the SPECT control subjects.

Volumes were calculated automatically using the FreeSurfer image analysis suite (http://surfer.nmr.mgh.harvard.edu/). A neuroradiologist (L.R.) reviewed individual scans, and those with significant artifact or motion disturbance were excluded from analysis. The automated procedures for volumetric measurements were as previously described [Fischl et al., 2002, 2004]. This procedure automatically provides segments and labels for various brain structures and assigns a label to each voxel on the basis of probabilistic information estimated automatically from a manually labeled set. The processing includes motion correction and averaging of multiple volumetric T1-weighted images, removal of non-brain tissue, automated Talairach transformation, segmentation of the subcortical white matter and deep gray matter volumetric structures (including the hippocampus, amygdala, caudate, putamen, thalamus, corpus callosum, brain stem, and CSF), intensity normalization, tessellation of the gray–white matter boundary, automated topology correction, and surface deformation. This technique has previously been shown to be comparable in accuracy to manual labeling [Fischl et al., 2002] and has been demonstrated to show good test–retest reliability across different scanner manufacturers and field strengths [Han et al., 2006]. Total volumes were

TABLE I. Demographics, Clinical, and Genetic Data of the Patients With a Diagnosis of SDS in Whom Imaging Was Performed

Patient number	Gender	Age of scanning (year)	Age of diagnosis (year)	School or work performance	Hematology symptoms	Pancreas insufficiency	SBDS mutations
1	F	26	4	Part-time job, school certificates	Mild aplastic anemia	Y	c.183_184TA>CT c.258 + 2T>C
2	M	23	1	Institutionalized	neutropenia	Y	c.183_184TA>CT c.258 + 2T>C
3[a]	M	18	2	Special education	Neutropenia	Y	c.297–300 del AAGA c.258 + 2T>C
4	M	18	4	Small volunteer job, school certificates	Neutropenia	Y	c.297–300 del AAGA c.258 + 2T>C
5	M	14	5	Special education	None	Y	c.183_184TA>CT c.258 + 2T>C
6	F	12	3	Special education	Neutropenia	Y	c.183_184TA>CT c.258 + 2T>C

[a]In this case, the MRI could not be analyzed accurately due to movement artifacts.

calculated as the sum of the left and right volumes, if applicable, for each study participant.

DAT Imaging

All six cases participated in the DAT imaging session (Table I). We were able to compare the quantitative DAT data obtained in four of these cases (3 males and 1 female; mean age: 21 years, range: 17–26 years) with data obtained in a group of 15 healthy young adult controls (this group of healthy controls is not the same control group that was included for the MRI study).

Participants were examined using SPECT and the well-validated DAT tracer [^{123}I]FP-CIT [Booij et al., 1997]. In each participant, approximately 110 MBq (3 mCi) [^{123}I]FP-CIT (specific activity $\geq$ 185 MBq/nmol; radiochemical purity > 98%; produced by GE Healthcare, Eindhoven, The Netherlands) was injected intravenously as a bolus.

SPECT studies were always performed 3 hr after injection (a period in which the specific striatal binding ratios are stable [Booij et al., 1999]), using a 12-detector single slice brain-dedicated scanner (Neurofocus 810, which is an upgrade of the Strichmann Medical Equipment) with a full-width at half-maximum (FWHM) resolution of approximately 6.5 mm, throughout the 20 cm field-of-view (http://www.neurophysics.com). After positioning of the subjects with the head parallel to the orbitomeatal line, axial slices parallel and upward from the orbitomeatal line to the vertex were acquired in 5 mm steps. Each acquisition consisted of approximately 15 slices with 2.5 min scanning time per slice, acquired in a 64 × 64 matrix. The energy window was set at 135–190 keV.

Attenuation correction of all brain SPECT images was performed as described earlier [Booij et al., 1997]. Images were reconstructed in 3D mode. For quantification, a region-of-interest (ROI) analysis was performed. A standardized template of fixed ROIs for the whole striatum, caudate nucleus, and putamen bilaterally, and occipital cortex was used. The striatal ROIs were positioned on four consecutive axial slices with the highest striatal activity. In these slices, occipital binding was assessed as well, which was assumed to represent non-displaceable activity (nonspecific binding and free radioactivity). Finally, specific to nonspecific binding ratios were calculated as (activity in ROI minus non-specific binding/non-specific binding), and used as the outcome measure.

Statistical Analysis

Differences in age and gender between groups were analyzed with *t*-tests and Fisher test, respectively. Differences in brain volume and DAT binding ratios were analyzed using ANOVA. MRI volume analyses were statistically corrected for total intracranial volume. Statistical significance was defined as $P < 0.05$.

RESULTS

MR Imaging and Volumetry

Accurate MRI scans were obtained in five SDS patients. On visual inspection, all MRI scans were normal, for example, no signs of atrophy or abnormal white matter signal intensities. On our group-analysis, however, significant reductions in overall gray- and white-matter volume, in the order of 23% (Table II) in SDS patients, after

TABLE II. Structural MRI Analysis in SDS Patients and Controls

	Controls (n = 6)	SDS patients (n = 5)	% Difference	Chi-square and student *t*-test
Males/females	4/2	3/2		NS
Age (mean years ± SD)	16.2 (3.9)	18.3 (5.5)		NS
Volume (mean L ± SD)				**ANOVA** intracranial volume as covariate
Gray matter	0.64 (0.06)	0.49 (0.08)	−23	0.007
White matter	0.39 (0.04)	0.30 (0.05)	−23	0.028
CSF	0.06 (0.02)	0.12 (0.02)	50	0.011
Total volume	1.03 (0.01)	0.80 (0.01)	−22	0.005
Structural analysis (mean ml ± SD)				
Thalamus	15.63 (1.77)	12.72 (1.60)	−21	0.009
Caudate nucleus	7.20 (1.43)	6.54 (0.41)	−9	NS
Putamen	11.51 (0.60)	10.88 (0.61)	−5	NS
Pallidum	3.10 (0.42)	2.95 (0.26)	−6	NS
Amygdala	2.98 (0.42)	2.67 (0.38)	−10	NS
Hippocampus	7.53 (1.25)	7.14 (0.82)	−5	NS
Corpus callosum _anterior	0.93 (0.19)	0.80 (0.16)	−14	NS
Corpus calosum_mid anterior	0.76 (0.2)	0.49 (0.23)	−36	NS
Corpus callosum_central	0.80 (0.22)	0.46 (0.17)	−43	0.021
Corpus callosum_mid posterior	0.80 (0.26)	0.38 (0.06)	−53	0.02
Corpus callosum_posterior	1.26 (0.25)	0.67 (0.27)	−47	0.009
Brainstem	20.20 (3.00)	15.36 (2.01)	−24	0.017
Cerebellum gray matter	105.47 (4.95)	88.64(8.56)	−16	0.007
Cerebellum white matter	30.00 (3.72)	25.33 (6.10)	−16	NS

correcting for intracranial volume. In line with this, ventricular volume (CSF) was significantly higher (+50%) in the patients.

On our structural analysis, we observed significant smaller volumes particularly posteriorly and caudally located in the brain: the corpus callosum (corpus and splenium), brainstem, and cerebellum. In addition the thalamus was smaller in SDS patients (see Table II).

SPECT

We obtained accurate DAT SPECT imaging data from all 6 participating SDS patients. In all these cases, intense and symmetrical striatal FP-CIT binding was visualized (Fig. 1).

For statistical comparison the DAT SPECT imaging of 4 SDS cases could be matched for age- and gender with data obtained in a group of 15 healthy young adults (mean age: 22.2 ± 3.2 years, range: 18–28 years; 10 males). There were no statistically significant differences in age and gender between the group of four SDS cases and the group of healthy controls. In all of these cases and controls, the striatal uptake was quantitatively symmetrical. Therefore, the data will be presented as the mean of left and right sides. Specific to nonspecific binding ratios were statistically significantly higher in the SDS cases than in the controls. This was true for the whole striatum as well as for subregions of the striatum (i.e., caudate nucleus and putamen; Fig. 2; all *P*-values <0.01).

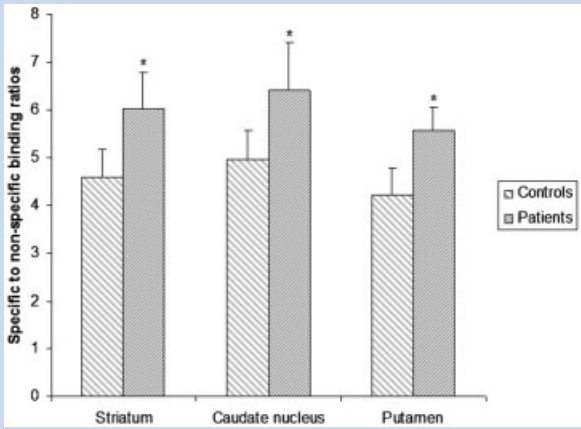

FIG. 2. Specific to nonspecific ratios of FP-CIT binding (reflecting DAT availability) for the whole striatum, caudate nucleus and putamen (average of both sides) obtained in four SDS patients and 15 age-matched healthy controls. Nonspecific binding was assessed in the occipital cortex (a brain area devoid of DATs). *Statistically significantly higher ratios in SDS than in controls (all *P* values <0.01).

DISCUSSION

In this study, we observed a significantly increased availability of striatal DAT binding in the brain of SDS patients. In addition, we replicated findings of decreased global brain volume, in which both gray and white matter volumes were reduced. The SDS patients had significantly smaller corpus callosum (corpus and splenium; the splenium is located posteriorly in the corpus callosum), brainstem, and cerebellum.

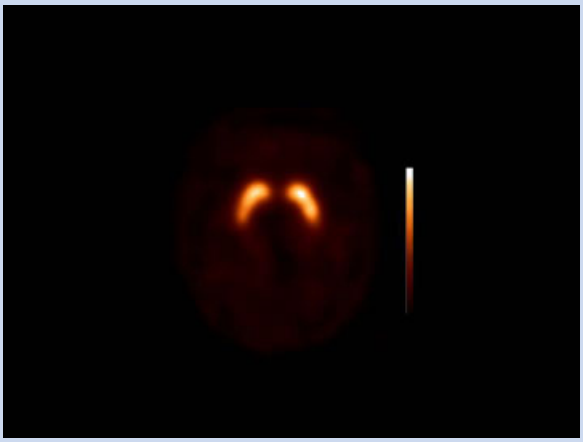

FIG. 1. Transversal SPECT slice at the level of the striatum obtained 3 hr after bolus injection of [^{123}I]FP-CIT in Patient 2 (Table I). Note the intense binding of FP-CIT to dopamine transporters both in the caudate nucleus and putamen bilaterally. [Color figure can be seen in the online version of this article, available at http://wileyonlinelibrary.com/journal/ajmga]

We were able to compare in vivo DAT data in SDS cases quantitatively with an age-matched control group. Due to ethical reasons we were not able to compare quantitatively the DAT data obtained in two young SDS cases with age-matched control data. However, also in these two younger cases, striatal uptake ratios were remarkably high. For instance, the caudate nucleus ratios of 8.6 and 7.9 were higher even than the mean observed for the young adult SDS cases (Fig. 2).

How could this novel finding on increased striatal DAT availability be interpreted? DAT binding is not synonymous with the number of nigrostriatal dopaminergic neurons. Consequently, an increased DAT availability may reflect an upregulation of DAT, for example, as a compensatory mechanism to increased synaptic dopamine concentrations. Alternatively, the increased DAT binding may be secondary to changes in other brain areas and/or neurotransmitter systems. The activity of midbrain dopaminergic neurons is regulated, in part, by glutamatergic projections from cortical areas acting via glutamatergic NMDA receptors [Laruelle et al., 2003]. An accurate functioning of neurocircuits involving functional connections between the (prefrontal) cortex and striatum are thought to play a major role in cognitive functions such as working memory and attention [Williams and Goldman-Rakic, 1995]. So, our present observation may be secondary to impaired glutamatergic projections from cortical brain areas. Alternatively, dopaminergic neurons projecting to the cortex and striatum are regulated by corticofugal glutamatergic neurons both directly and via GABAergic interneurons [Carlsson et al., 2001] in brain regions such as prefrontal cortex, striatum, and thalamus, so our present observation may

be secondary to impaired functioning of GABAergic interneurons. There are no studies that have examined the dopaminergic or other neurotransmission systems in SDS, but our finding may encourage future studies to look into these systems in SDS, particularly since recent imaging studies showed associations between striatal DAT availability and learning processes on the one hand [Mozley et al., 2001; Berger et al., 2004] and ADHD on the other [Dougherty et al., 1999].

The clinical presentation in SDS may differ among patients. Some patients live independently, have a regular job or were only diagnosed in adulthood. Although learning and ADHD may be the more common denominators in SDS, some individuals may present relatively normal, while carrying the same *SBDS* gene mutations as commonly identified. The variation in the learning capacity is further indicated by the living circumstances of the patients included in the current study.

In line with the literature, total brain volume, global gray and white matter volumes and specific brain volumes were consequently smaller in SDS patients than in age-matched controls. In contrast to a study by Toiviainen-Salo et al. [2008] in which mainly posteriorly located brain regions were analyzed, we also analyzed other brain regions (e.g., amygdala, hippocampus, thalamus, caudate nucleus, putamen, and pallidum). Whereas Toiviainen-Salo et al. suggested that the majority of the measured brain structures were smaller, we confirm that this observation holds true in our patients for the brain regions located in the posterior fossa (cerebellum and brainstem) and corpus callosum. This is of particular interest in view of the reported behavioral problems, and cognitive dysfunction, including learning difficulties in SDS patients [Toiviainen-Salo et al., 2008; Kerr et al., 2010]. Cerebellum and corpus callosum, in addition to the thalamus, are brain structures well known to play a role in learning difficulties. Many of our SDS cases showed learning difficulties, as 4 out of 6 have received or are still following special educational programs or need institutional support (Table I).

Our observation of reduced GM and WM volumes are somewhat different from those previously reported by Toiviainen-Salo et al. [2008], in which GM and WM reductions in SDS patients were proportionally reduced to their head size (no difference was found after correcting for intracranial volume). This indicates that we found even more reduced GM and WM volumes than in the study by Toivianen-Salo and co-workers. We included younger patients than Toivianen-Salo and co-workers did. One explanation for the discrepancy in brain volumes might be that volume differences in SDS might be more prone at a younger age. Alternatively, we may have included patients that were more affected than those in the report of Toivianen-Salo, although we have no evidence for this assumption. Regarding brain functioning in SDS, no measures of severity are as yet available, apart from behavioral issues as has only recently been quantified. Finally, this difference may also be caused by statistical chance due to the small number of patients studied, both in the present study and that of Toiviainen-Salo et al. [2008].

How could we link the presently observed nigrostriatal dopaminergic and structural abnormalities? The structural MRI data point to smaller brain regions in SDS, particularly posteriorly located in the brain. It is of interest that in ADHD, a well known neurodevelopment disorder of children characterized by inattention symptoms, the results of 2 meta-analyses indicated a smaller posterior part of the corpus callosum (splenium; as assessed by morphometric MRI) in ADHD patients versus age- and gender-matched controls [Valera et al., 2007; Hutchinson et al., 2008]. Also, another MRI technique is able to asses the integrity of white matter tracts (this technique is called diffusion tensor imaging; DTI). The corpus callosum is the main white matter tract of the brain, and a recent DTI study showed a reduced integrity of this tract again localized in a posterior part of the corpus callosum in ADHD [Cao et al., 2010]. So, structural and functional abnormalities in posterior parts of the corpus callosum may suggest that the quantity of interhemispheric connections are fewer; that is, abnormalities in the specific corresponding region of the brains from where these fibers originate, in this case the sensory–motor cortex. Indeed, a recent meta-analysis indicated aberrant activation of sensory–motor cortex during cognitive tasks in ADHD [Dickstein et al., 2006]. Finally, functional glutamatergic NMDA receptors are expressed throughout the human cortical brain areas [Erlandsson et al., 2003], and callosotomy in rats leads to changes of glutamate and GABA in presynaptic terminals in cortical areas [Marcano-Reik et al., 2010].

Although speculative, our data may point to abnormal glutamatergic projections associated with volume loss of posterior parts of the corpus callosum, and secondary changes of the nigrostriatal pathways, which is reflected by an increase of DAT binding in the striatum, which may be associated with cognitive dysfunctions in SDS such as learning difficulties. Of course, our study cannot prove causality.

Our study has some limitations. First, the number of participants is relatively low. Therefore, our findings need replication. Second, in future studies it would be of interest to link the imaging findings directly to results of neuropsychological tests [Perobelli et al., 2012]. Third, all SDS patients received enzyme replacement and water-soluble vitamins for their pancreas insufficiently. However, it is not likely that such medications will influence DAT binding significantly [Booij and Kemp, 2008]. Finally, while SPECT and MRI data were both obtained in 6 SDS patients, SPECT and MRI data were not obtained in the same group of healthy age-matched controls.

In conclusion, our data replicate earlier findings on smaller brain regions in SDS. In addition, our novel molecular imaging data suggest that SDS patients may have a dysregulated dopaminergic system. This finding, when replicated and directly compared with neuropsychological data, may be of relevance to increase our understanding of behavioral and cognitive deficits in SDS.

REFERENCES

Austin KM, Gupta ML, Coats SA, Tulpule A, Mostoslavsky G, Balazs AB, Mulligan RC, Daley G, Pellman D, Shimamura A. 2008. Mitotic spindle destabilization and genomic instability in Shwachman–Diamond syndrome. J Clin Invest 118:1511–1518.

Berger HJ, Cools AR, Horstink MW, Oyen WJ, Verhoeven EW, van der Werf SP. 2004. Striatal dopamine and learning strategy-an ^{123}I-FP-CIT SPECT study. Neuropsychologia 42:1071–1078.

Boocock GR, Morrison JA, Popovic M, Richards N, Ellis L, Durie PR, Rommens JM. 2003. Mutations in SBDS are associated with Shwachman–Diamond syndrome. Nat Genet 33:97–101.

Booij J, Tissingh G, Boer GJ, Speelman JD, Stoof JC, Janssen AG, Wolters EC, van Royen EA. 1997. [^{123}I]SPECT shows a pronounced decline of striatal labelling in early and advanced Parkinson's disease. J Neurol Neurosurg Psychiatry 62:133–140.

Booij J, Hemelaar TG, Speelman JD, de Bruin K, Janssen AG, van Royen EA. 1999. One-day protocol for imaging of the nigrostriatal dopaminergic pathway in Parkinson's disease by [^{123}I]FPCIT SPECT. J Nucl Med 40:753–761.

Booij J, de Jong J, de Bruin K, Knol R, de Win MM, van Eck-Smit BL. 2007. Quantification of striatal dopamine transporters with ^{123}I-FP-CIT SPECT is influenced by the selective serotonin reuptake inhibitor paroxetine: A double-blind, placebo-controlled, crossover study in healthy control subjects. J Nucl Med 48:359–366.

Booij J, Kemp P. 2008. Dopamine transporter imaging with [^{123}I]FP-CIT SPECT: Potential effects of drugs. Eur J Nucl Med Mol Imaging 35: 424–438.

Booij J, van Amelsvoort T, Boot E. 2010. Co-occurrence of early-onset Parkinson disease and 22q11.2 deletion syndrome: Potential role for dopamine transporter imaging. Am J Med Genet Part A 152A:2937–2938.

Cao Q, Sun L, Gong G, Lv Y, Cao X, Shuai L, Zhu C, Zang Y, Wang Y. 2010. The macrostructural and microstructural abnormalities of corpus callosum in children with attention deficit/hyperactivity disorder: A combined morphometric and diffusion tensor MRI study. Brain Res 1310:172–180.

Carlsson A, Waters N, Holm-Waters S, Tedroff J, Nilsson M, Carlsson ML. 2001. Interactions between monoamines, glutamate, and GABA in schizophrenia: New evidence. Annu Rev Pharmacol Toxicol 41:237–260.

Dickstein SG, Bannon K, Castellanos FX, Milham MP. 2006. The neural correlates of attention deficit hyperactivity disorder: An ALE meta-analysis. J Child Psychol Psychiatry 47:1051–1062.

Dougherty DD, Bonab AA, Spencer TJ, Rauch SL, Madras BK, Fischman AJ. 1999. Dopamine transporter density in patients with attention deficit hyperactivity disorder. Lancet 354:2132–2133.

Dror Y, Donadieu J, Koglmeier J, Dodge J, Toiviainen-Salo S, Makitie O, Kerr E, Zeidler C, Shimamura A, Shah N, et al. 2011. Draft consensus guidelines for diagnosis and treatment of Shwachman–Diamond syndrome. Ann N Y Acad Sci 1242:40–55.

Erlandsson K, Bressan RA, Mulligan RS, Gunn RN, Cunningham VJ, Owens J, Wyper D, Ell PJ, Pilowsky LS. 2003. Kinetic modelling of [^{123}I]CNS 1261–a potential SPET tracer for the NMDA receptor. Nucl Med Biol 30:441–454.

Finch AJ, Hilcenko C, Basse N, Goyenechea B, Menne TF, González Fernández A, Simpson P, D'Santos CS, Arends MJ, Donadieu J, et al. 2011. Uncoupling of GTP hydrolysis from eIF6 release on the ribosome causes Shwachman–Diamond syndrome. Genes Dev 25:917–929.

Fischl B, Salat DH, Busa E, Albert M, Dieterich M, Haselgrove C, van der Kouwe A, Killiany R, Kennedy D, Klaveness S, et al. 2002. Whole brain segmentation: Automated labeling of neuroanatomical structures in the human brain. Neuron 33:341–355.

Fischl B, Salat DH, van der Kouwe AJ, Makris N, Segonne F, Quinn BT, Dale AM. 2004. Sequence-independent segmentation of magnetic resonance images. Neuroimage 23:S69–S84.

Han X, Jovicich J, Salat D, van der Kouwe A, Quinn B, Czanner S, Busa E, Pacheco J, Albert M, Killiany R, et al. 2006. Reliability of MRI derived measurements of human cerebral cortical thickness: The effects of field strength, scanner upgrade and manufacturer. Neuroimage 32: 180–194.

Huang JN, Shimamura A. 2010. Clinical spectrum and molecular pathophysiology of Shwachman–Diamond syndrome. Curr Opin Hematol November 30, 2010 [Epub ahead of print].

Hutchinson AD, Mathias JL, Banich MT. 2008. Corpus callosum morphology in children and adolescents with attention deficit hyperactivity disorder: A meta-analytic review. Neuropsychology 22:341–349.

Kerr EN, Ellis L, Dupuis A, Rommens JM, Durie PR. 2010. The behavioral phenotype of school-age children with Shwachman–Diamond syndrome indicates neurocognitive dysfunction with loss of Shwachman–Bodian–Diamond syndrome gene function. J Pediatr 156:433–438.

Klingberg T. 2010. Training and plasticity of working memory. Trends Cogn Sci 14:317–324.

Kuijpers TW, Alders M, Tool AT, Mellink C, Roos D, Hennekam RC. 2005. Hematologic abnormalities in Shwachman–Diamond syndrome: Lack of genotype–phenotype relationship. Blood 106:356–361.

Laruelle M, Kegeles LS, Abi-Dargham A. 2003. Glutamate, dopamine, and schizophrenia: From pathophysiology to treatment. Ann N Y Acad Sci 1003:138–158.

Marcano-Reik AJ, Prasad T, Weiner JA, Blumberg MS. 2010. An abrupt developmental shift in callosal modulation of sleep-related spindle bursts coincides with the emergence of excitatory–inhibitory balance and a reduction of somatosensory cortical plasticity. Behav Neurosci 124: 600–611.

Mozley LH, Gur RC, Mozley PD, Gur RE. 2001. Striatal dopamine transporters and cognitive functioning in healthy men and women. Am J Psychiatry 158:1492–1499.

Narla A, Ebert BL. 2010. Ribosomopathies: Human disorders of ribosome dysfunction. Blood 155:3196–3205.

Orelio C, Verkuijlen P, Geissler J, van den Berg TK, Kuijpers TW. 2009. SBDS expression and localization at the mitotic spindle in human myeloid progenitors. PLoS ONE 4:e7084.

Orelio C, Kuijpers TW. 2009. Shwachman–Diamond syndrome neutrophils have altered chemoattractant-induced F-actin polymerization and polarization characteristics. Haematologica 94:409–413.

Orelio C, van der Sluis RM, Verkuijlen P, Nethe M, Hordijk PL, van den Berg TK, Kuijpers TW. 2011. Altered intracellular localization and mobility of SBDS protein upon mutation in Shwachman–Diamond syndrome. PLoS ONE 6:e20727.

Perobelli S, Nicolis E, Assael BM, Cipolli M. 2012. Further characterization of Shwachman–Diamond syndrome: Psychological functioning and quality of life in adult and young patients. Am J Med Genet Part A 158A:567–573.

Toiviainen-Salo S, Mäkitie O, Mannerkoski M, Hämäläinen J, Valanne L, Autti T. 2008. Shwachman–Diamond syndrome is associated with structural brain alterations on MRI. Am J Med Genet Part A 146A: 1558–1564.

Valera EM, Faraone SV, Murray KE, Seidman LJ. 2007. Meta-analysis of structural imaging findings in attention-deficit/hyperactivity disorder. Biol Psychiatry 61:1361–1369.

Williams GV, Goldman-Rakic PS. 1995. Modulation of memory fields by dopamine D1 receptors in prefrontal cortex. Nature 376: 572–575.

Yamaguchi M, Fujimura K, Kanegane H, Toga-Yamaguchi H, Chopra R, Okamura N. 2011. Mislocalization or low expression of mutated Shwachman–Bodian–Diamond syndrome protein. Int J Hematol 94: 54–62.